Superexchange interaction in K_2NiF_4: an ab initio Hartree-Fock study

1995 J. Phys.: Condens. Matter 7 7997

(http://iopscience.iop.org/0953-8984/7/41/009)

J. Phys.: Condens. Matter 7 (1995) 7997–8007. Printed in the UK

Superexchange interaction in K_2NiF_4: an *ab initio* Hartree–Fock study

R Dovesi†, J M Ricart‡, V R Saunders§ and R Orlando†

† Department of Inorganic, Physical and Materials Chemistry, University of Torino, via P Giuria 5, I-10125 Torino, Italy

‡ Department of Chemistry, Universitat Rovira i Virgili, Plaza Imperial Tarraco 1, 43005-Tarragona, Spain

§ Daresbury Laboratory, Daresbury, Warrington WA4 4AD, UK

Received 10 May 1995

Abstract. The ground-state electronic structures of the ferromagnetic and antiferromagnetic phases of K_2NiF_4 have been investigated using the *ab initio* periodic Hartree–Fock approach. The system is a wide-gap insulator. The antiferromagnetic phase is more stable than the ferromagnetic phase by 0.0216 eV per Ni pair, which is almost exactly two thirds of that found in $KNiF_3$, in agreement with the hypothesis of additivity of the superexchange interaction with respect to the number of Ni–Ni neighbours. K_2NiF_4 turns out to be a two-dimensional antiferromagnet, the calculated interlayer superexchange interaction being at least three orders of magnitude smaller than that within the layers; the latter is shown to obey a d^{-12} (d is the shortest Ni–Ni distance) power law as suggested in the literature, and as verified in a previous study on $KNiF_3$. The two apical F ions of the NiF_6 octahedra not involved in the Ni–F–Ni superexchange path play an important role in determining the ferromagnetic–antiferromagnetic energy difference, which on the other hand is insensitive to large geometrical modifications that leave the octahedra unaltered. Charge- and spin-density maps are used to illustrate the electronic structure of the system and the superexchange mechanism.

1. Introduction

K_2NiF_4 has been the subject of considerable experimental [1–5] and theoretical [6–9] interest because of both its peculiar properties and its structural similarity to La_2CuO_4, the prototype of high-T_c cuprate superconductors. K_2NiF_4 is an antiferromagnetic insulator, with a Néel temperature T_N of 97 K. Its structure (see figure 1) consists of NiF_2 layers separated by two KF layers; the space group is D_{4h}^{17} ($I4/mmm$). In the basal plane, Ni is fourfold coordinated with a Ni–Ni distance of 4.01 Å and a Ni–F–Ni angle of 180°. The distance between the Ni planes along the c axis is large ($c/2$, where c = 13.08 Å; table 1), so that K_2NiF_4 is usually considered to be a two-dimensional antiferromagnet. The local situation around the Ni atoms is very similar to that in cubic $KNiF_3$ perovskite; the NiF_6 octahedron, which is regular in $KNiF_3$ (Ni–F distance equal to 2.01 Å), is only slightly distorted in K_2NiF_4 (2.00 and 1.97 Å for the equatorial and the apical F, respectively). However, in $KNiF_3$ there are six second-nearest neighbours, compared to only four in K_2NiF_4. Various experimental data [1–4], analysed by de Jongh and Block [7] in terms of the magnetic coupling constants J, indicate that $KNiF_3$ and K_2NiF_4 possess very similar J-values ($-J/k$ ranges from 44 to 51 K for $KNiF_3$ and from 48 to 52 K for K_2NiF_4, where k is the Boltzmann constant).

0953-8984/95/417997+11$19.50

In the present paper we explore the electronic and magnetic properties of K_2NiF_4 using an *ab initio* quantum-mechanical method and compare them with the corresponding quantities in $KNiF_3$. In particular the total energy of the ferromagnetic (FM) and antiferromagnetic (AFM) ground states are evaluated as a function of the geometrical parameters. This allows us

(i) to compare the J-value calculated from ΔE, the FM–AFM energy difference, with those resulting from experiment,

(ii) to compare the calculated J dependence on the Ni–Ni distance d with that inferred from experimental data [7],

(iii) to verify the additivity of the superexchange Ni–F–Ni interactions with respect to the number of metal–metal neighbours, as assumed in model Hamiltonians, such as the Ising or the Heisenberg models,

(iv) to discuss the relative importance of the intra-plane and inter-plane magnetic coupling constants (J and J', respectively) and

(v) to discuss the role of the apical F ions, which are not involved in a superexchange interaction.

The electronic structure analysis is complemented with electron charge-density and spin-density maps and structural data. In a parallel paper the electronic structure of $KNiF_3$ has been investigated [10].

2. Computational method

The implementation of the *ab initio* self-consistent field (SCF) Hartree–Fock LCAO computational scheme for periodic systems within the CRYSTAL code [11] has been described in previous papers [12, 13]. Recent additions to the code were used for calculations of the FM and AFM states within the unrestricted Hartree–Fock theory; information on the implementation and on the results referring to simple transition-metal oxides can be found in [14] and in [15, 16], respectively. There are three main limitations to the accuracy of calculations using this scheme. The main source of error, electron correlation, comes directly from the Hartree–Fock approximation. In previous work, this has generally led to an underestimate of the binding energies by about 30% [17, 18], and to overestimates of the lattice parameter for transition-metal compounds of approximately 2% [14–16]. Functionals of the Hartree–Fock density (see for example [19, 20]) have been shown to be very effective in correcting the binding energies [17, 18], and to correct in the right direction (about 10% increase) the AFM–FM energy difference, which in the case of $KNiF_3$ [10] is underestimated by about 40% at the Hartree–Fock level.

The second source of inaccuracy may come from the numerical approximations introduced in the implementation of the SCF equations. These approximations appear in the reciprocal-space integration and in the evaluation of Coulomb and exchange series. In this work, high numerical accuracy was achieved using values of 7, 7, 7, 7 and 14 for the parameters controlling the direct-space summations [11–13]. The reciprocal-space integration was performed by sampling the Brillouin zone at a regular set of points defined by a shrinking factor IS of 4 (21 k-points in the irreducible part of the Brillouin zone); the energy difference with respect to a calculation performed with IS= 8 is less than 10^{-6} Hartree/cell. In order to reduce numerical noise, all the calculations have been performed with the AFM double cell; the energy difference for the FM state between calculations with the single and the double cell is less than 10^{-7} Hartree/cell, however.

The third source of error relates to the choice of basis set. Extended Gaussian basis sets

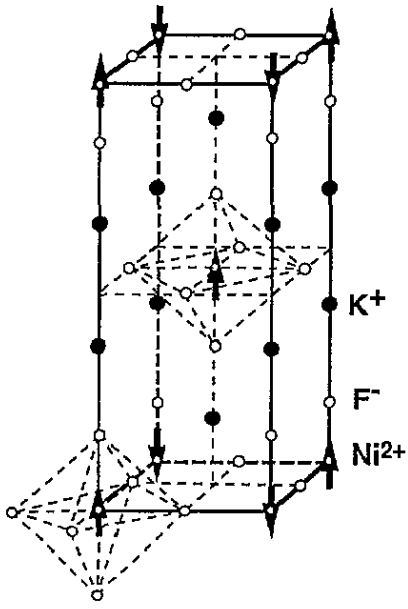

Figure 1. The crystal structure of K_2NiF_4. The arrows indicate the Ni spin orientations in the AFM structure.

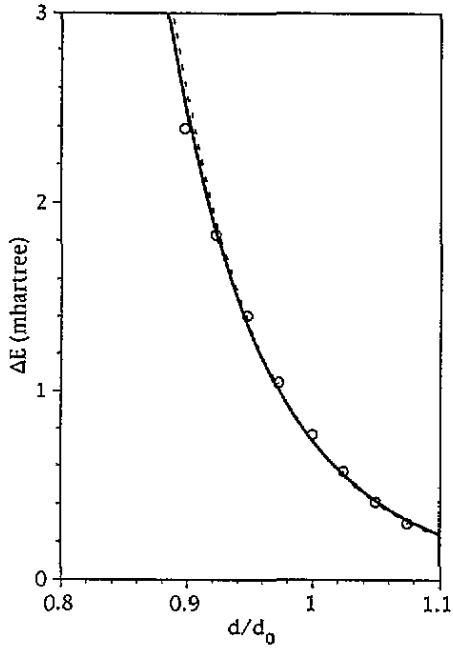

Figure 2. Energy difference per two formula units between the FM and AFM phases as a function of d, the in-plane Ni–Ni distance. The NiF_6 octahedron is regular (Ni–F distance equal to $d/2$, c is kept constant at the experimental value; z_F, the fractional coordinate of the apical F atoms, is varied to maintain the regularity of the octahedron). The broken line is two thirds of the FM–AFM energy difference for $KNiF_3$. d_0 is the experimental d-value (4.01 Å). For the interpolating curve, see text.

composed of 27, 17 and 13 'atomic orbitals' have been used for Ni, K and F, respectively, where each orbital is a linear combination (contraction) of Gaussian-type functions. The basis set has been optimized (exponents and coefficients) in previous studies (see [16], [21] and [22] for Ni, K and F, respectively). Larger basis sets (d functions on K and F; a 5-1G contraction for the Ni d shell, instead of the 4-1G contraction of [16], with a more diffuse outer Gaussian which provides a larger Ni–F–Ni overlap; addition of a diffuse sp shell on Ni) have been used for single-point calculations in the parallel study of $KNiF_3$ [10], where it has been shown that ΔE, the FM–AFM energy difference, changes by less than 1% as a consequence of these basis set improvements.

3. Results and discussion

3.1. The structural data

The calculated geometrical parameters and bulk modulus are given in table 1, together with the available experimental data. The a lattice parameter is overestimated by about 2%, in line with the results for $KNiF_3$ [10], MnO and NiO [14–16]. The overestimation of c

is larger (3.4%), because the interaction between the NiF_2 and KF layers is weak, with a non-negligible contribution from dispersion forces (which are disregarded at the Hartree–Fock level) and because the Hartree–Fock method tends to overestimate the size of heavy cations (K^+ in the present case), as indicated by the results for the series Li_2O, Na_2O, K_2O [21] and LiF, NaF, KF [23]. The resulting error for the equilibrium volume is +7%. The bulk modulus is small (less than one third of that of $KNiF_3$), as a consequence of the large compressibility along the *c* axis.

Table 1. Calculated and experimental equilibrium geometry and bulk modulus B, lattice parameters *a* and c, fractional coordinates of Z_F and Z_K. The numbers in parentheses are the percentage errors with respect to experiment.

	Calculated value	Experimental value
a (Å)	4.08 (+1.75)	4.01
c (Å)	13.52 (+3.36)	13.08
c/*a*	3.313	3.26
V	225.1 (+7.03)	210.3
z_F	0.152	0.151
z_K	0.352	0.352
B (GPa)	49.2	—

3.2. The magnetic properties

In the present study we considered the FM state, the non-magnetic NM state and two different antiferromagnetic (AFM and AFM′) states. The spin ordering for AFM is shown in figure 1; each Ni atom in a NiF_2 plane is surrounded by four Ni atoms of opposite spin. The situation is similar to that in $KNiF_3$ [10] where, however, the number of neighbours is six instead of four. The in-plane Ni–Ni distance is 4.01 Å in both cases. The AFM′ structure is a sequence of (001) FM planes with opposite spin. The difference with respect to the FM situation is that Ni atoms belonging to different planes have opposite spin (they are third nearest Ni–Ni neighbours; the Ni–Ni distance is 7.13 Å; there are eight such neighbours for each Ni atom). At the experimental geometry the energy difference between the AFM′ and FM solutions is less than 10^{-5} eV/cell (this is the threshold above which we consider our energy differences reliable), showing that the inter-plane superexchange interaction is extremely small. The AFM solution, on the contrary, is more stable than the FM solution by 0.0216 eV per Ni pair, and more stable than the NM solution by many electronvolts. This energy ordering remains unchanged when relatively large geometry modifications are performed (compression or expansion of *c*, keeping *a* constant; compression of *a* at constant *c*; variation in z_F at constant volume; isotropic compression), although obviously the energy differences are changing as a function of these modifications, as will be discussed below.

In their recent study with a local-density functional approach, Eyert and Hock [9] found an energy difference between the AFM and the NM states of only 0.3 eV, whereas their FM state is less stable than the NM state. Small orthorhombic deformations of the double cell were sufficient to alter the energy order and to cause a transition from an insulator to a metallic state. This unrealistic picture is due presumably to the poor description of the exchange operator at the local-density level, which plays a crucial role in the definition of the position of d states in the band structure.

The energy difference ΔE between the FM and the AFM states can be related to the experimental data obtained with various techniques [1–4]; the experimental results are

usually expressed in terms of the magnetic coupling constants J of a model (Heisenberg or Ising) spin Hamiltonian. The intra-planar 'experimental' J-values, collected by de Jongh and Block [7], range from -48 to -52 K (in Boltzmann's constant units) for K_2NiF_4 and from -44 to -51 K for $KNiF_3$. J', the interlayer magnetic coupling constant, is estimated to be 10^4–10^6 times smaller than J [7]. If we refer to the Ising model (which is in some sense more appropriate than the Heisenberg model, because our Hartree–Fock solutions are eigenvectors of S_z and not of S^2), the following relation holds between J and ΔE:

$$\Delta E = 2S^2 Jz \tag{1}$$

where z is the number of Ni second neighbours (four in K_2NiF_4) and S is the total spin moment ($S = 1$ in the present case). The resulting calculated $-J$-value is 31.3 K, between 60 and 65% of the experimental value. The agreement, although semiquantitative, is very satisfactory, if we take into account the state of the art in this field and the very small energy differences involved. The 40% quantitative discrepancy may be attributed to many factors such as

(i) correlation effects, which are disregarded at the Hartree–Fock level,

(ii) spin–orbit terms, not included in the present calculation,

(iii) inadequacy of the models adopted in going from the experimental measured quantity to J, and/or from the calculated ΔE to J through the Ising model and

(iv) spin contamination of our $S = 1$ and $S = 0$ states.

Let us turn now to the problem of the additivity of the superexchange interactions, which is implicit in the Ising (factor z in equation (1)) as well as in the Heisenberg model. The calculated ΔE-values for $KNiF_3$ ($z = 6$) and K_2NiF_4 ($z = 4$) are 0.030 83 and 0.021 58 eV at the experimental geometries, and their ratio $r = 1.43$ is very close to the theoretical value, 6/4. If the K_2NiF_4 octahedron is given exactly the same geometry as in $KNiF_3$ (Ni–F distance equal to 2.005 Å), the ratio increases to $r = 1.48$. The scaling with the number of neighbours remains nearly constant (between 1.48 and 1.51) for a large range of Ni–F distances, which corresponds to a variation in J by about one order of magnitude, as shown in figure 2, where ΔE as a function of the Ni–F distance is reported for the two systems. The K_2NiF_4 data have been obtained by modifying the side of the *perfect* NiF_6 octahedra by keeping c fixed at the experimental value. In figure 2 the calculated points are interpolated with a power law of the Ni–Ni distance:

$$\Delta E = K(d/d_0)^n \tag{2}$$

where d_0 is the experimental a lattice parameter. It turns out that for both systems the exponent is around -12 (-11.5 and -12.3 for K_2NiF_4 and $KNiF_3$, respectively) as proposed by de Jongh and Block [7] on the basis of the analysis of the experimental J-values for $XNiF_3$ and X_2NiF_4 compounds with different lattice parameters.

There are other aspects of the superexchange interaction that can be investigated within the present model. We can explore how ΔE is perturbed by the position of the K^+ ions and by the relative position of the (unaltered) octahedra. In figure 3 the broken curve gives ΔE as a function of c when the octahedra are kept at their experimental geometry. The figure shows that ΔE changes by less than 2% when c is varied from 13 to 18 Å; it should be noticed that the corresponding variation in the total energy is close to 2 eV per formula unit, which is about four orders of magnitude more than ΔE; this clearly shows that the surroundings of the NiF_6 octahedra have only a minor influence on the superexchange interaction, also for relatively large modifications of the crystalline structure. A related question concerns the role of the apical F ions in the superexchange interaction and determining the magnitude of

Table 2. Spin population (in electrons) of the valence 'atomic orbitals' in the FM and AFM solutions. 'Inner' and 'Outer' refer to the internal and external (most diffuse) valence functions on the given atoms; 'Total' is the sum of the two contributions; in the case of the FM solution the sum of all the spin populations in the unit cell is 2 electrons; in the AFM case, only one Ni atom is reported; the second Ni atom has opposite spin populations.

		Spin population (electrons)					
		FM			AFM		
		Inner	Outer	Total	Inner	Outer	Total
F equatorial	p_x	0.026	−0.010	0.016	0.000	0.000	0.000
F equatorial	p_y, p_z	0.002	−0.002	0.000	0.000	0.000	0.000
F apical	p_z	0.016	−0.004	0.012	0.016	−0.004	0.012
F apical	p_x, p_y	0.001	−0.001	0.000	0.001	−0.001	0.000
Ni	d_{z^2}	0.851	0.111	0.962	0.851	0.111	0.962
Ni	$d_{x^2-y^2}$	0.851	0.118	0.969	0.851	0.117	0.968
Ni	d_{xz}, d_{yz}, d_{xy}	0.021	−0.020	0.001	0.021	−0.020	0.001

ΔE. The full curve in figure 3 shows ΔE as a function of c with the fractional coordinate of the apical F ions kept fixed, i.e. when the Ni–F_{ap} distance is changing proportionally to c. In this case the ΔE variation is much larger, with a decrease of about 25% from the value at the experimental geometry and this effect can be interpreted in terms of decreased compression of the Ni ion, and in particular of its d-electron charge distribution; when the apical F ions are at a larger distance, the d-electron charge distribution can contract in the basal plane and expand in the z direction, reducing the Ni–F–Ni superexchange coupling. In order to take into account this effect, equation (2) above can be generalized as follows:

$$\Delta E = A[(2z_F/d)^m - C](d/d_0)^n \tag{3}$$

where z_F is the z coordinate of the apical fluorine atoms. In the regular octahedra $2z_F = d$, so that in figure 2 the quantity in square brackets in equation (3) is constant ($K = A[1-C]$, where K is the constant in equation (2)). In figure 3 (full curve), $d = d_0$. The data in figures 2 and 3 have been used to fit the above equation; the resulting parameters are $A = 0.173\,73$ mHartree; $C = -3.356\,88$; $m = -8.057\,99$; $n = -11.510\,67$; the m exponent is then smaller than n.

If the unit cell is now compressed in the basal plane keeping c (and the z_{ap} fractional coordinate) fixed at the experimental value, the points shown in figure 4 are obtained; the full curve is obtained from equation (3). In this case the increase in ΔE under the in-plane compression is less dramatic than for the regular octahedra, because the system can reduce the exchange repulsion in the FM state by slightly expanding the d-electron charge distribution in the z direction, as discussed above.

3.3. The electronic structure

K_2NiF_4 is a fully ionic insulator. The *net charges*, evaluated according to a Mulliken scheme, are very close to the formal charges (+1.00, +1.87 and −0.96 for K, Ni and F, respectively, in both the FM and the AFM solutions). The Ni d population corresponds to that of a d^8 atomic configuration (8.09 electrons, for both the FM and the AFM solutions). The excess is due to overlap terms with neighbouring atoms. The population of the three

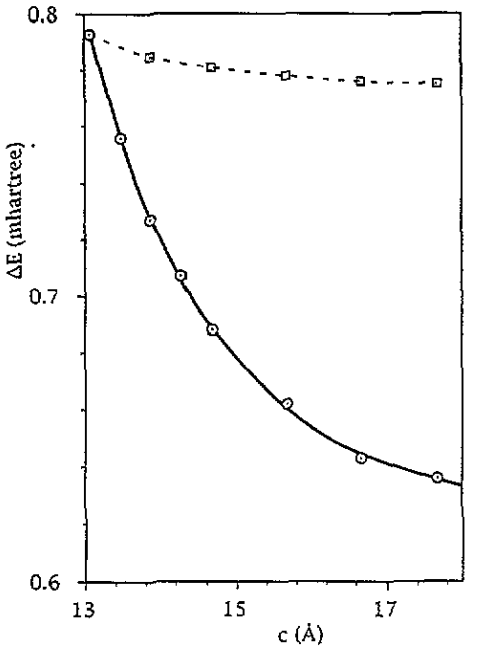

Figure 3. Energy difference (per two formula units) between the FM and AFM phases as a function of the lattice parameter c. The full and broken curves refer to calculations in which the position of the apical F ions (and then the amount of distortion of the NiF_6 octahedron) remains constant, or changes proportionally to c, respectively. The a lattice parameter is kept at the experimental value (4.01 Å).

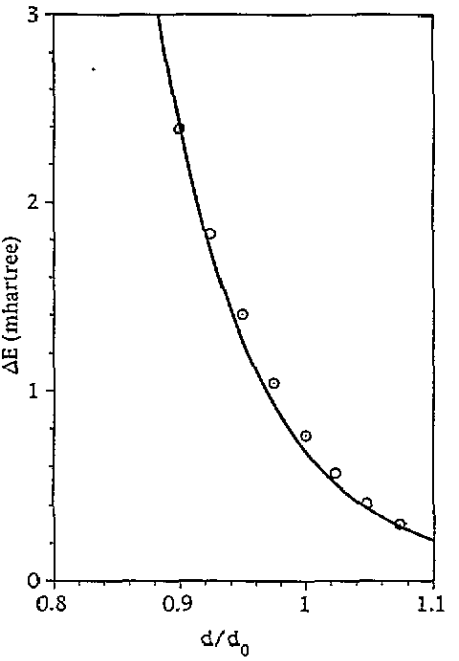

Figure 4. Energy difference (per two formula units) between the FM and AFM phases as a function of d, the in-plane Ni–Ni distance. The lattice parameter c and the fractional coordinate z_F are fixed at the experimental value. d_0 is the experimental d-value (4.01 Å). For the interpolating curve, see text.

degenerate t_{2g} d orbitals is exactly 2, while that of the two e_g d orbitals is slightly larger than 1. The apical F ions are not symmetry equivalent to the equatorial ions, but the corresponding atomic charges and multipoles are very similar. The fully ionic structure of K_2NiF_4 is confirmed by the Mulliken bond populations. We recall that large positive bond populations indicate covalent bonds; very small or null bond populations mean the absence of a covalent bond, such as in ionic compounds. Finally, negative bond populations indicate short-range (exclusion) repulsion. In the present case the bond populations are zero (Ni–K) or very small and negative (−0.004 and −0.013 electrons for the Ni–F and K–F bonds, respectively). This picture is confirmed by the charge-density maps shown in figures 5 and 6. In particular the difference maps (bulk minus superposition of spherical ionic charge distributions) show

(a) for Ni, depletion of charge (chain lines) along the principal axes, and build-up of charge along the 'diagonals' (direction of d_{xy}, d_{xz} and d_{yz}),

(b) for F, depletion along the Ni–F–Ni line, and transfer of this charge in the orthogonal direction and

(c) for K (see the (100) section) a typical ionic spherical contraction.

As regards the spin atomic densities, the Ni atomic spin is close to 2 (1.95 electrons for both the FM and the AFM states) and is entirely due to the d orbitals. The spin polarization

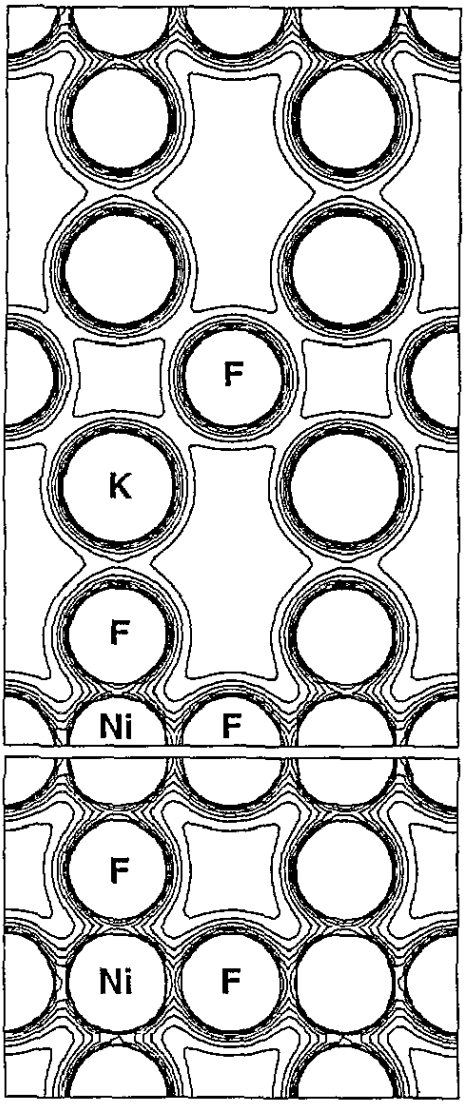

Figure 5. Total charge-density map in the (001) plane (bottom) through the Ni and F atoms, and in a (100) plane (top) through the three types of atom. The separation between contiguous isodensity curves is 0.01 electrons Bohr^{-3}; the innermost curves in the atomic region correspond to 0.08 electrons Bohr^{-3}.

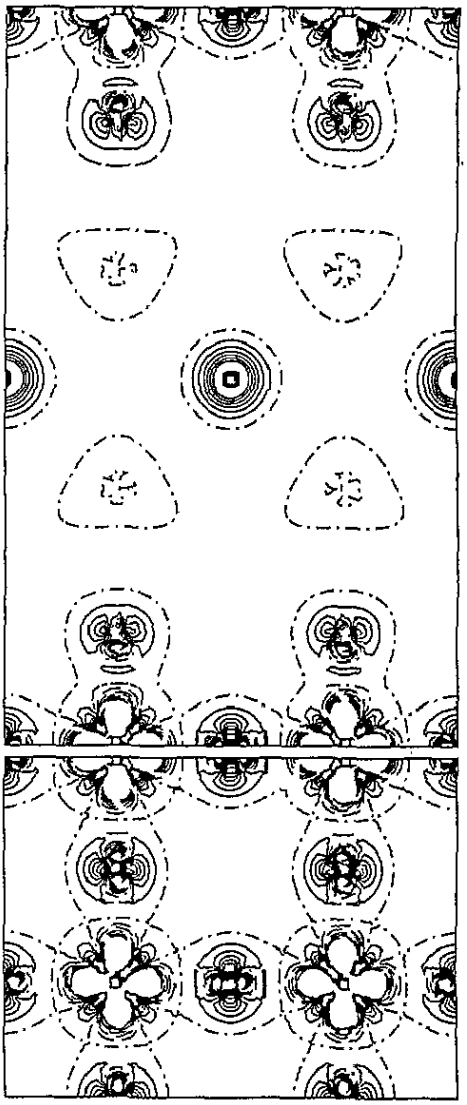

Figure 6. Difference charge-density maps. Sections as in the previous figure. The difference between the bulk density and the density obtained as a superposition of ions is reported. The ionic solutions have been obtained with the same basis sets used for the periodic calculations. The separation between contiguous isodensity curves is 0.005 electrons Bohr^{-3}. The function is truncated in the core regions at $\pm$0.03 electrons Bohr^{-3}. The full, broken and chain lines correspond to positive, negative and zero values, respectively.

does not involve the K^+ ions at all (atomic spin 0.00 electrons), as is clearly shown in figure 7 (top). A small net spin density is located on the equatorial and apical F atoms

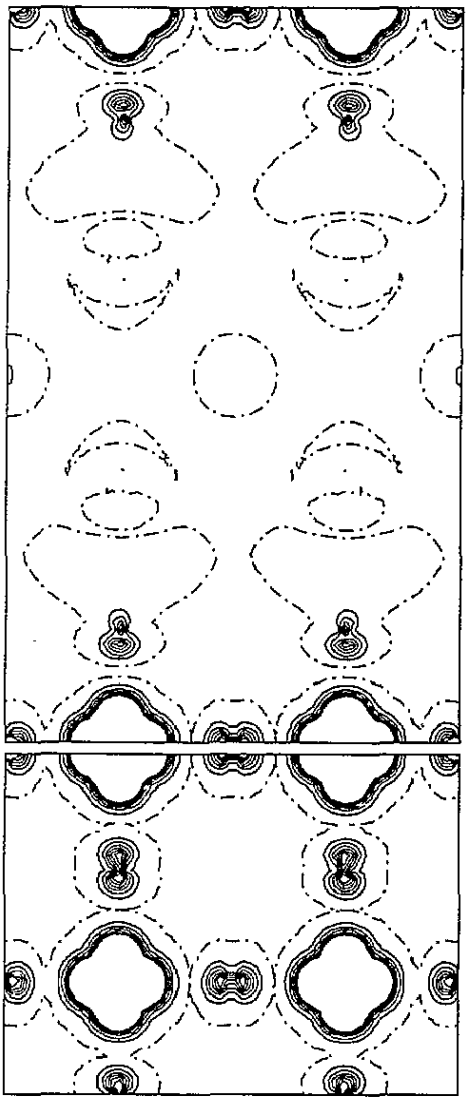

Figure 7. Spin-density maps for the FM solution; sections, symbols and scale as in previous figure.

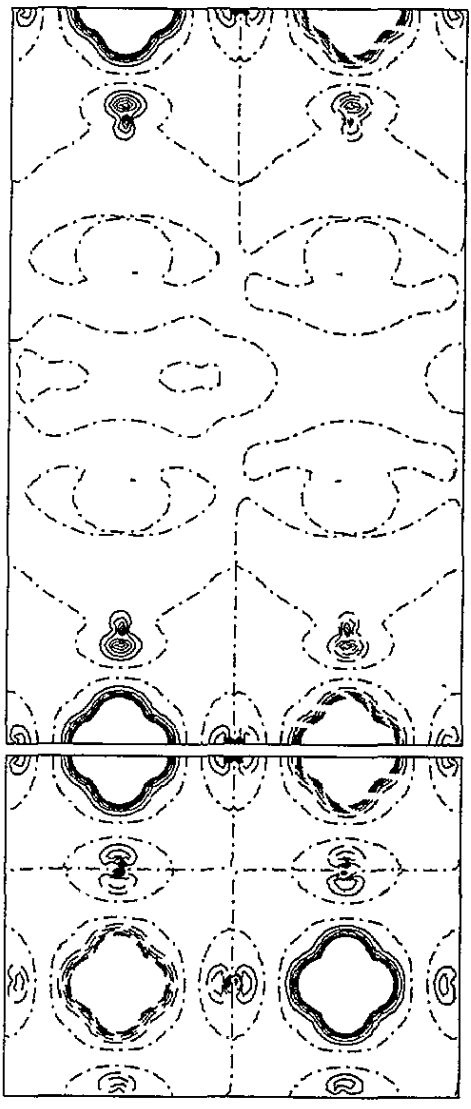

Figure 8. Spin-density maps for the AFM solution; sections, symbols and scale as in figure 6.

in the FM case (0.016 and 0.012 electrons, respectively); the former disappears because of symmetry reasons in the AFM solution, and the latter remains unaltered. The FM and AFM charge- and spin-density distributions are very similar (see figures 7 and 8 for the spin density). The only difference is the extra build-up of charge and spin density on the equatorial F atoms in the FM solution compared to the AFM solution.

The crucial point for understanding the larger stability of the AFM state with respect to the FM state is the small spin polarization and charge distribution contraction on the F atoms. The superexchange mechanism in the present case acts as follows: due to the fully ionic nature of this compound, the ions when 'inserted' in the solid contract to some amount

in order to reduce the Pauli (or exchange, or short-range) repulsion in the ion–ion contact region. This is clearly shown in figure 5. On the F ions, the contraction is more marked for the α electrons than for the β in the FM solution, because of the two unpaired α electrons on the two neighbouring Ni atoms. In the AFM case the reduction in the short-range repulsion is easier, because it can be obtained with a small shift in the α electrons towards the Ni atom with β polarization, and vice versa. This simple mechanism is confirmed not only by figures 7 and 8 but also by the data in table 2, where the populations of some atomic orbitals on the Ni and F atoms are given. The table shows firstly that the FM and the AFM values are very similar in all but one case, the p_x spin population of the in-plane F atoms, which is null in the AFM solution and not in the FM solution, and secondly that this spin population is positive (same sign as the Ni atoms) in the 'inner' atomic orbitals, i.e. in the F core region, and negative in the 'outer' region, i.e. in the region of the atom–atom repulsion, which confirms the interpretation of a transfer of α electrons from the Ni–F region (so that in that region there is an excess of β electrons of the F-closed shell) to the core region, with a consequence of build-up of α spin density as appears in figure 7. The corresponding negative or β spin density does not appear in the maps because firstly it is much more diffuse, so that it is not evident in this scale, and secondly it should appear in the Ni–F direction where, however, the Ni α spin density dominates (two electrons, whereas the F polarization is of the order of 0.02 electrons).

The system is a wide-band-gap insulator; the general features of DOS are very similar to those of $KNiF_3$, which have been reported in [10].

4. Conclusions

The Hartree–Fock method describes correctly, at least on a qualitative level, the ground-state electronic properties of K_2NiF_4. The system is a two-dimensional antiferromagnet. The calculated magnetic coupling constant J is about 60% of the experimental value. The additivity of the superexchange interaction has been verified by comparing the results for $KNiF_3$ (six Ni–Ni interactions) and K_2NiF_4 (four interactions). The calculated J dependence on d, the Ni–Ni distance, is well fitted by a d^{-x} power with $x = 11.5$, in very good agreement with the value estimated by de Jongh and Block [7] comparing the experimental J-values for systems with similar geometries but different Ni–Ni distances. The role of the apical F ions has been discussed. The higher stability of the AFM phase with respect to the FM phase has been interpreted in terms of short-range repulsion and has been documented with charge-density maps and orbital population data.

Acknowledgments

Financial support from CSI Piemonte and from the Italian Ministero dell'Università e della Ricerca Scientifica e Tecnologica (MURST, 60%) is gratefully acknowledged. RD wishes to thank the Universitat Rovira i Virgili (Tarragona) for a 2 month grant. The work was supported by the Human Capital and Mobility Programme of the European Community under contract CHRX-CT93-0155, by the CICyT project PB92-0766-C02-02 of the Spanish Ministerio de Educacion y Ciencia and the CIRIT project GRQ93-7.003 of the Generalitat de Catalunya.

References

[1] de Jongh L J and Miedema A R 1974 *Adv. Phys.* **23** 1
[2] de Jongh L J 1973 *AIP Conf. Proc.* **10** 561
[3] de Wijn H W, Walker L R and Walstedt R F 1973 *Phys. Rev.* B **8** 285
[4] Skalyo J Jr, Shirane G, Birgeneau R J and Guggenheim H J 1969 *Phys. Rev. Lett.* **23** 1394
[5] Birgeneau R J, Guggenheim H J and Shirane G 1970 *Phys. Rev.* B **1** 2211
[6] Lines M E 1967 *Phys. Rev.* **164** 736
[7] de Jongh L J and Block R 1975 *Physica* B **79** 568
[8] Hatta S, Kasowski R V and Hsu W Y 1992 *J. Appl. Phys.* **72** 4480
[9] Eyert V and Hock K H 1993 *J. Phys.: Condens. Matter* **5** 2987
[10] Ricart J M, Dovesi R, Saunders V R and Roetti C 1995 *Phys. Rev.* B **52** 2381
[11] Dovesi R, Pisani C, Roetti C, Causà and Saunders V R 1989 *CRYSTAL88, QCPE program N.577* (Bloomington, IN: Quantum Chemistry Program Exchange, Indiana University))
Dovesi R, Saunders V R and Roetti C 1992 *CRYSTAL92 User's Manual* (Torino: Gruppo di Chimica Teorica, Università di Torino)
[12] Pisani C, Dovesi R and Roetti C 1988 *Lecture Notes in Chemistry* vol 48 (Heidelberg: Springer)
[13] Saunders V R, Freyria-Fava C, Dovesi R, Salasco L and Roetti C 1992 *Mol. Phys.* **77** 629
[14] Aprà E 1993 *PhD Thesis* Università di Torino
[15] Mackrodt W C, Harrison N M, Saunders V R, Allan N L, Towler M D, Aprà E and Dovesi R 1993 *Phil. Mag.* A **68** 653
[16] Towler M D, Allan N L, Harrison N M, Saunders V R, Mackrodt W C and Aprà E 1994 *Phys. Rev.* B **50** 5041
[17] Dovesi R, Roetti C, Freyria-Fava C, Aprà E, Saunders V R and Harrison N M 1992 *Phil. Trans. R. Soc.* A **341** 203
[18] Causá M, Dovesi R and Roetti C 1991 *Phys. Rev.* B **43** 11937
[19] Perdew J P 1986 *Phys. Rev.* B **33** 8822 (Errata 1986 *Phys. Rev.* B **34** 7407)
[20] Perdew J P, Chevary J A, Vosko S H, Jackson K A, Pederson M R, Singh D J and Foilhais C 1992 *Phys. Rev.* B **46** 6671
[21] Dovesi R, Roetti C, Freyria-Fava C, Prencipe M and Saunders V R 1991 *Chem. Phys.* **156** 11
[22] Catti M, Dovesi R, Pavese A and Saunders V R 1991 *J. Phys.: Condens. Matter* **3** 4151
[23] Prencipe M, Zupan A, Aprà E, Dovesi R and Saunders V R 1995 *Phys. Rev.* B **51** 3391